Supporting Information

Small molecule delivery to solid tumors with chitosan-coated PLGA particles: A lesson learned from comparative imaging

Jinho Park, Yihua Pei, Hyesun Hyun, Mark A. Castanares, David S. Collins, Yoon Yeo*

a

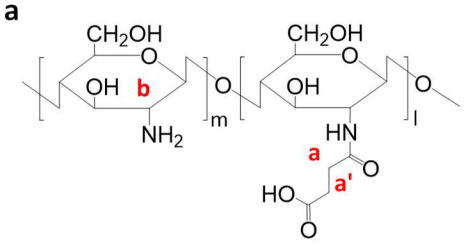

b

An/Am	a, a'	b	m	l	% amidation
0.1	0.51	1.06	1.06	0.127	10%
0.3	5.26	3.3	3.3	1.31	28%

m = b
l = (a, a')/4
% amidation = l/(m+l)

c

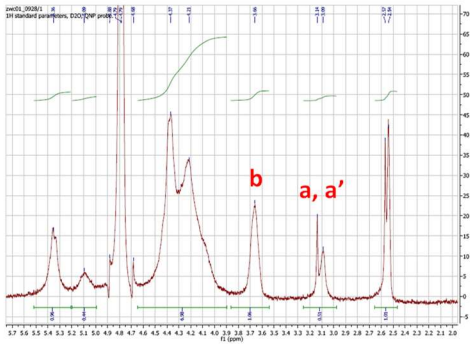

d

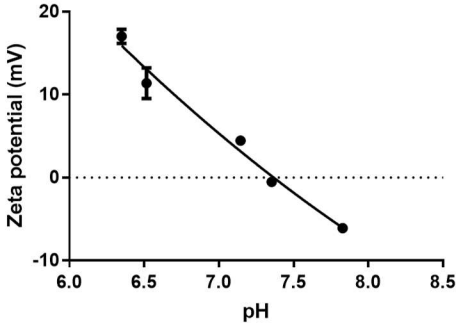

Supporting Fig. 1. (a) ZWC structure; (b) % Degree of succinylation of ZWC calculated from H^1NMR; (c) H^1NMR spectrum of $ZWC_{0.1}$ (solvent: 2% CD_3COOD in D_2O, at 70 °C); (d) Zeta potential of $ZWC_{0.1}$ at different pHs.

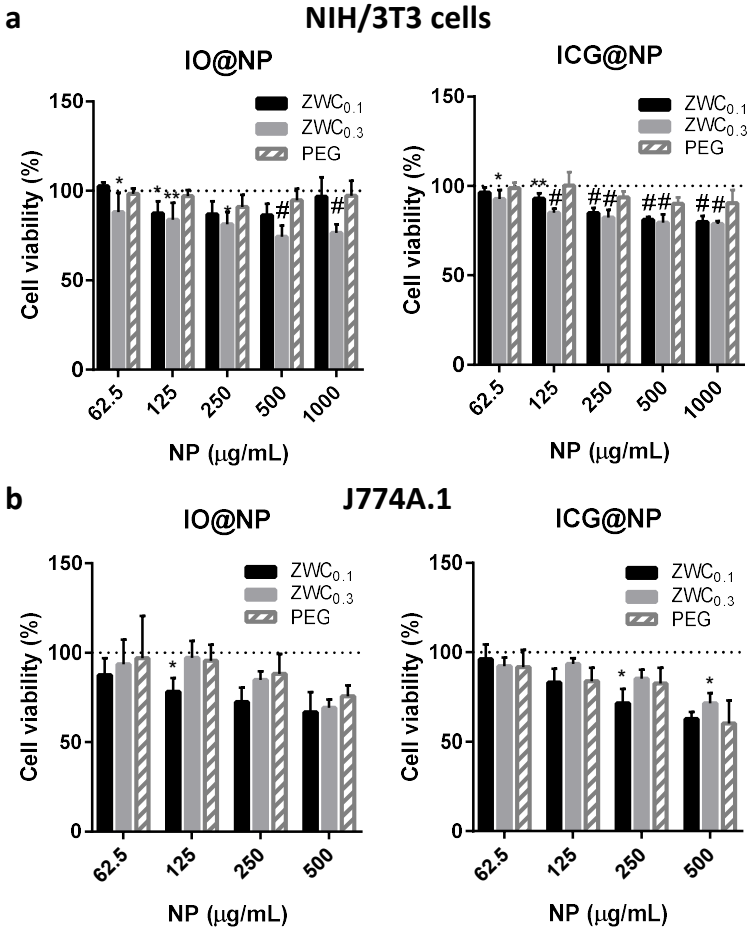

Supporting Fig. 2. Cytocompatibilty of NPs after 1 day incubation in (a) NIH3T3 fibroblasts and (b) J774A.1 macrophages. Cell viability (%) = Absorbance of formazan formed in treated cells / formazan absorbance of control cells with no treatment. Dotted line: Cell viability of control cells. n=5 replicates. *: $p<0.05$; **: $p<0.01$; #: $p<0.001$ vs. NP-pD-PEG by Dunnett's multiple comparisons test.

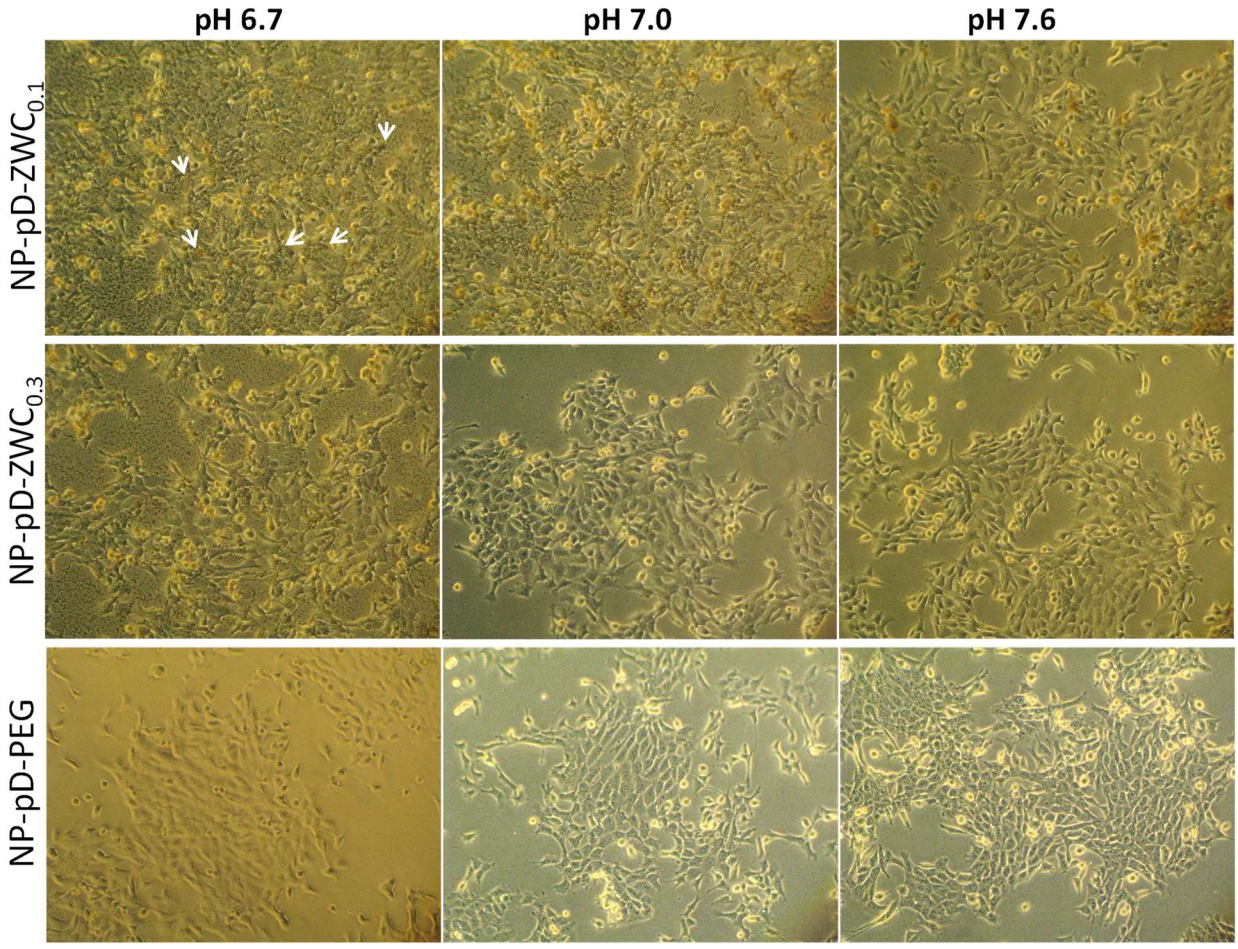

Supporting Fig. 3. 4T1 cell images after incubation with surface-modified NPs for 4 h and washing with fresh medium to remove loosely bounded NPs. NP-pD-ZWC$_{0.1}$ remained with cells and wells at pH 6.7 and pH 7.0, and NP-pD-ZWC$_{0.3}$ persisted likewise at pH 6.7. White arrows show examples of aggregated NPs bound to cells.

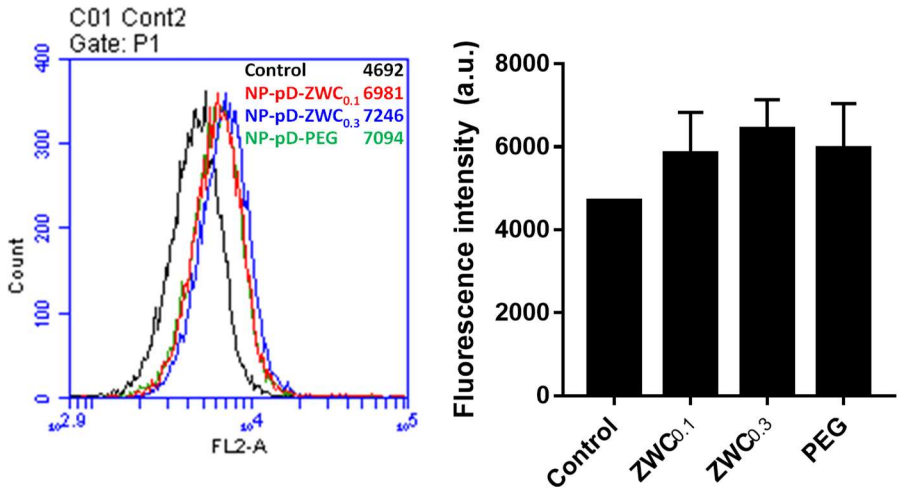

Supporting Fig. 4. A representative flow cytometry histogram of J774A.1 macrophages treated with surface-modified Rho-NPs. n=3 independently prepared samples.

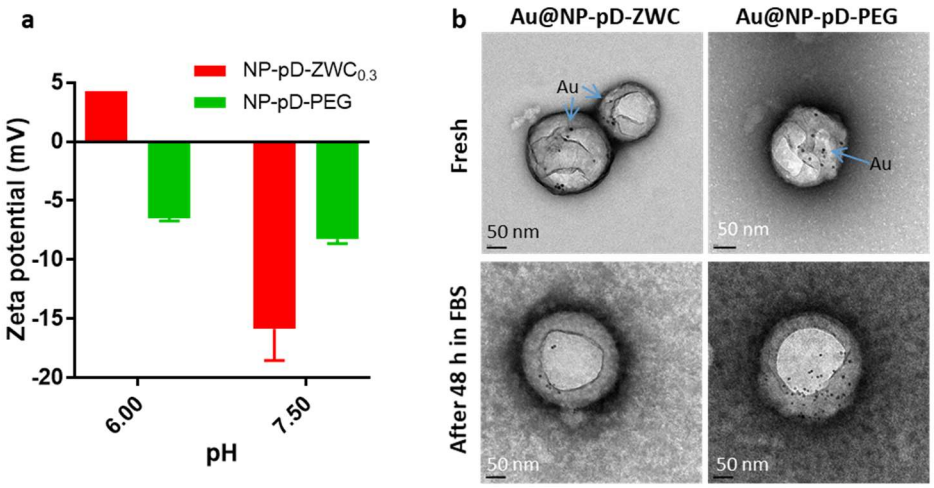

Supporting Fig. 5. (a) Zeta potential of surface-modified Au@NPs at different pHs. (b) TEM images of surface-modified Au@NPs. Scale bars: 50 nm.

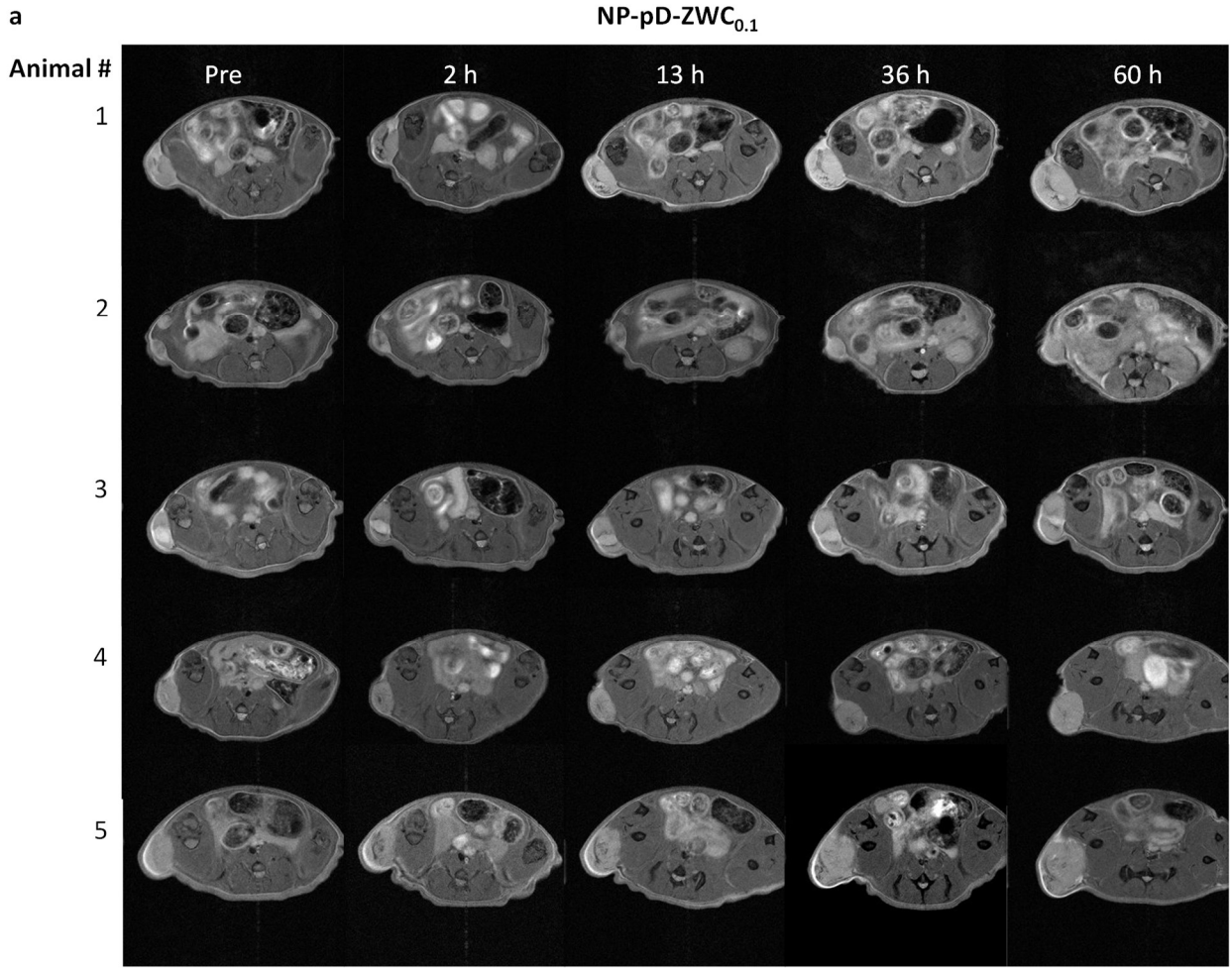

Supporting Fig. 6. (a) T2-weighted MR images of LS174T tumors before and after the treatment with (a) IO@NP-pD-ZWC$_{0.1}$.

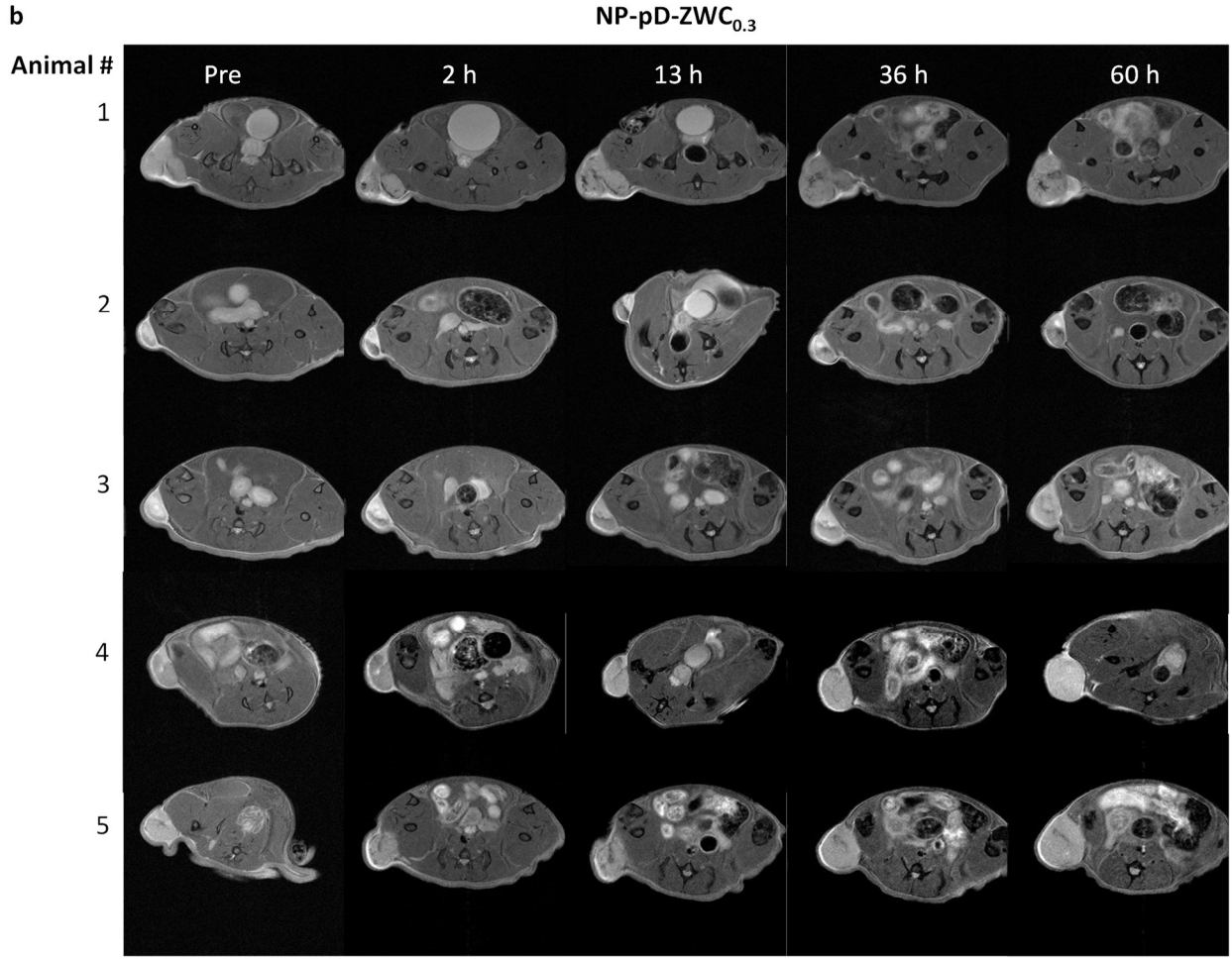

Supporting Fig. 6. (b) T2-weighted MR images of LS174T tumors before and after the treatment with (b) IO@NP-pD-$ZWC_{0.3}$.

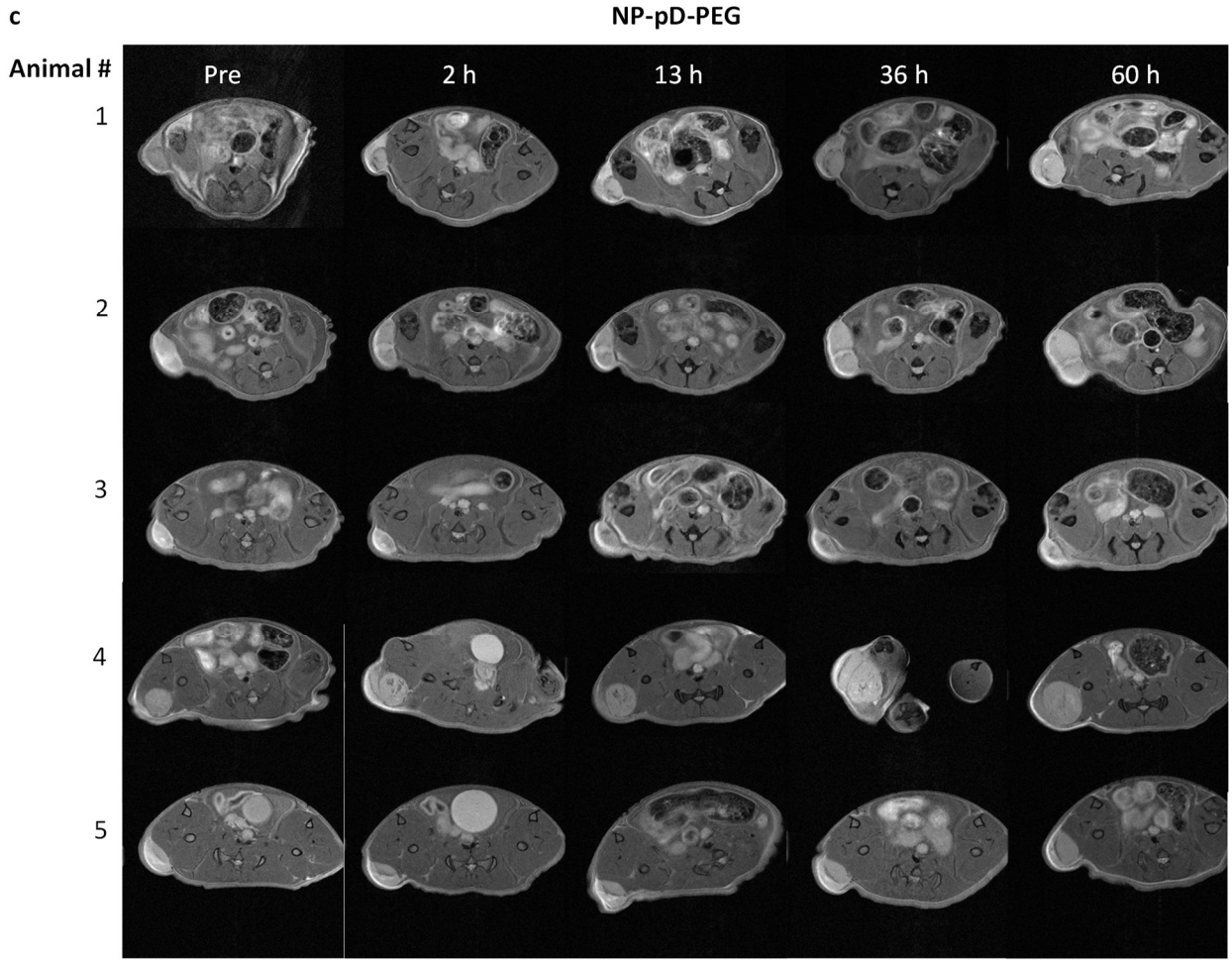

Supporting Fig. 6. (c) T2-weighted MR images of LS174T tumors before and after the treatment with (c) IO@NP-pD-PEG.

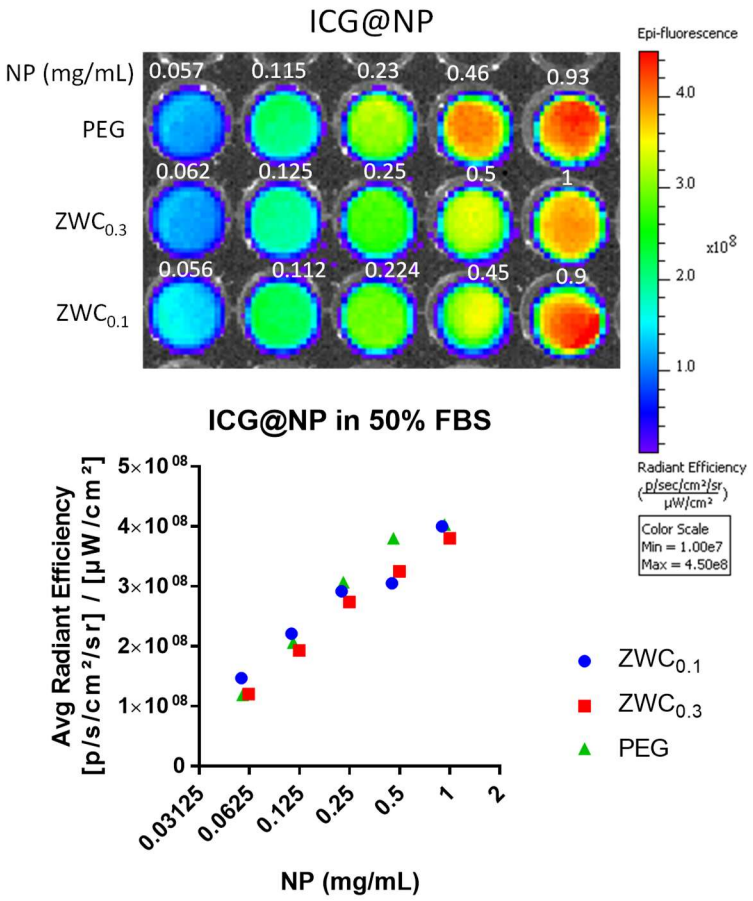

Supporting Fig. 7. ICG fluorescence intensity of ICG@NPs in 50% FBS. n=3 measurements of a representative batch.

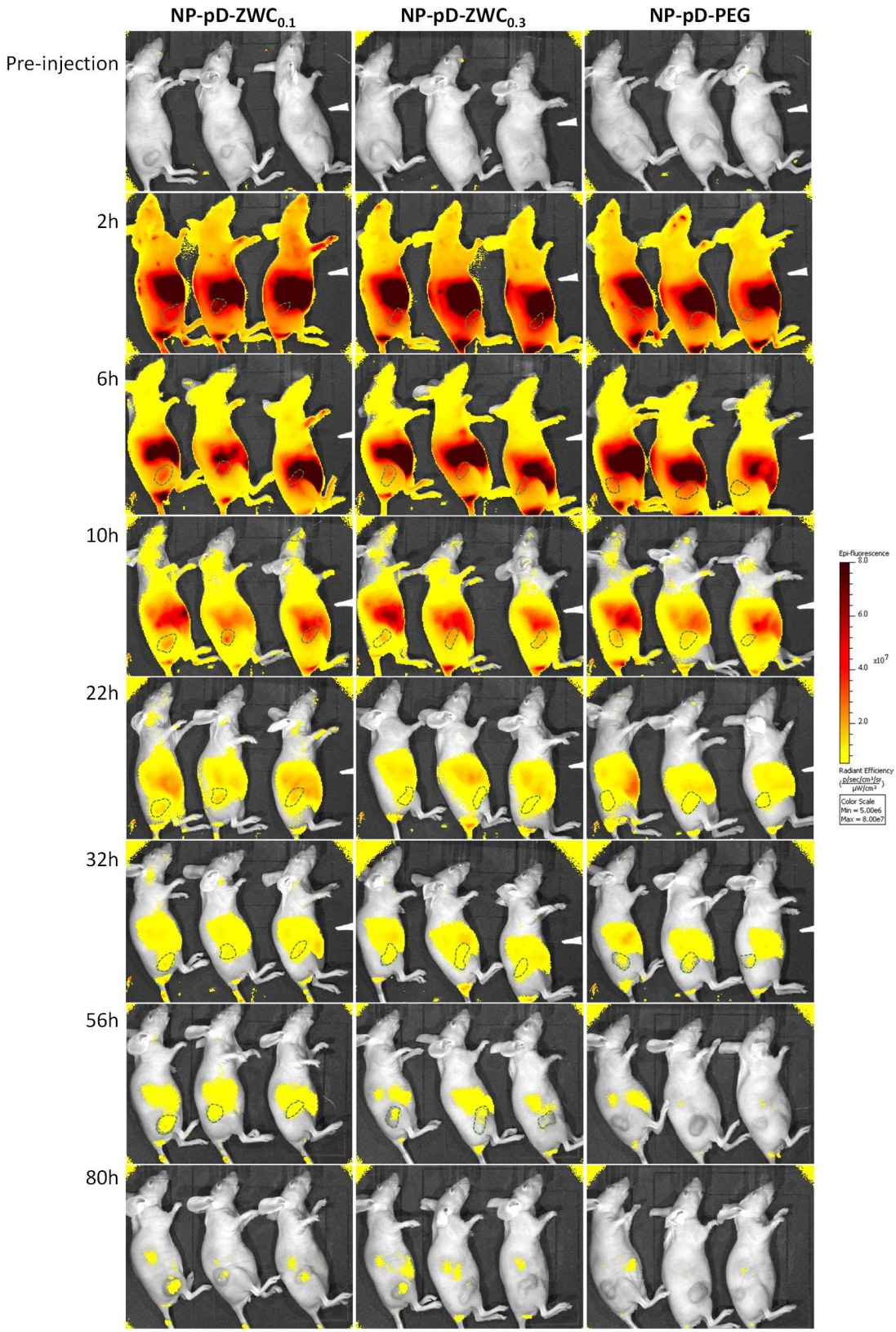

Supporting Fig. 8. IVIS images of LS174T tumor-bearing animals treated with (a) IO@NP-pD-ZWC$_{0.1}$, (b) IO@NP-pD-ZWC$_{0.3}$, and (c) IO@NP-pD-PEG .

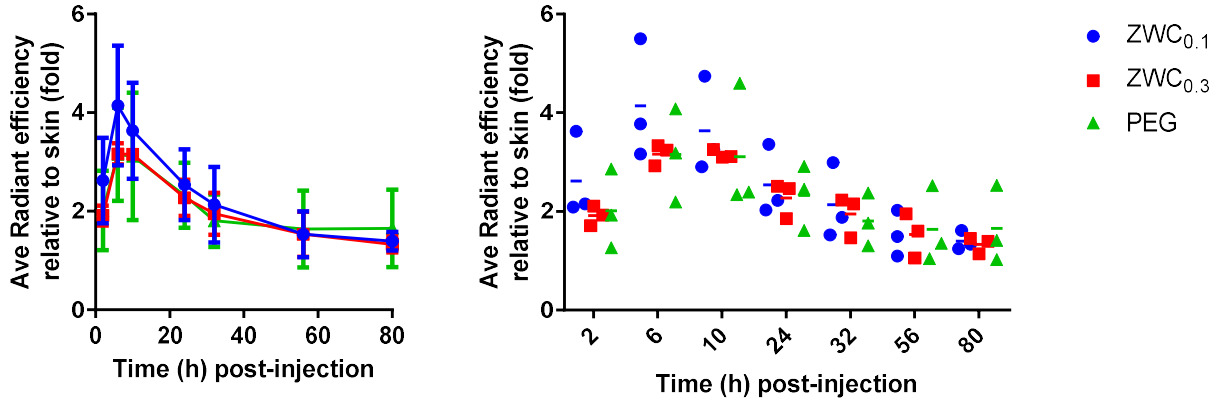

Supporting Fig. 9. Radiant efficiency of tumor area relative to the skin of the shoulder front at each time point in two different representations (2nd independently performed study. n=3 per treatment, average ± standard deviation).

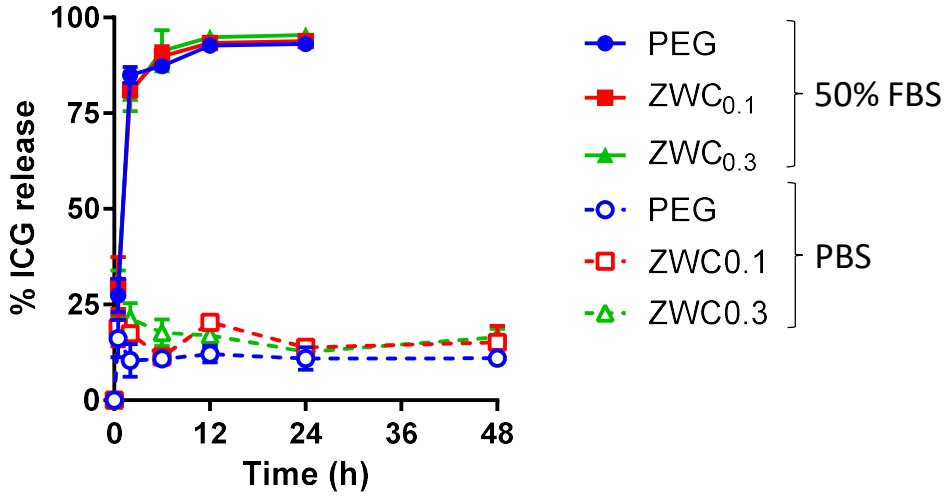

Supporting Fig. 10. ICG release from ICG@NPs in 50% FBS vs. PBS. n=3 replicates per sample. ICG@NPs were incubated in 50% FBS/PBS or PBS at a concentration of 0.2 mg/mL. At predetermined time points, NPs were centrifuged at 9200 rcf for 15 min to separate a supernatant and a pellet. The supernatant and the pellet were resuspended in 50% FBS (for NPs incubated in 50% FBS) or 50% ACN (for NPs incubated in PBS), placed in a black 96-well plate and imaged with an IVIS Lumina II system (PerkinElmer, MA).

Supporting Table. pH of LS174T tumors measured with a Mettler Toledo InLab solid electrode in animals under isofluorane anesthesia.

Organs	pH	
	Mouse 1	Mouse 2
Tumor (330 mm^3)	7.1-7.2	Not determined
Tumor (>1700 mm^3)	6.70-7.12	7.07-7.08
Abdominal cavity	7.39-7.40	7.38
Liver	7.34-7.40	7.25
Blood	7.39-7.42	7.38
Heart	7.33-7.45	7.34